Astron. Astrophys. 315, L101–L104 (1996)

ASTRONOMY AND ASTROPHYSICS

# SWS spectroscopy of the colliding galaxies NGC 4038/39⋆

**D. Kunze**[1], **D. Rigopoulou**[1], **D. Lutz**[1], **E. Egami**[1], **H. Feuchtgruber**[1,2], **R. Genzel**[1], **H.W.W. Spoon**[1], **E. Sturm**[1] **A. Sternberg**[3], **A.F.M. Moorwood**[4], **and Th. de Graauw**[5]

[1] Max-Planck-Institut für Extraterrestrische Physik, Postfach 1603, D-85740 Garching, Germany
[2] ISO Science Operations Centre, Astrophysics Division of ESA, Apdo. 50727, E-28080 Villafranca/Madrid, Spain
[3] School of Physics and Astronomy and The Wise Observatory, Tel Aviv University, Tel Aviv 69978, Israel
[4] European Southern Observatory, Karl-Schwarzschild-Str. 2, D-85748 Garching, Germany
[5] Space Research Organization of the Netherlands and Kapteyn Institute, P.O. Box 800, 9700 AV Groningen, The Netherlands

Received 17 July 1996 / Accepted 13 August 1996

**Abstract.** We present mid-infrared spectroscopy of the prototypical interacting galaxies NGC 4038/39 (the 'Antennae') obtained with the ISO Short Wavelength Spectrometer (SWS). Our observations focus on the interaction zone where the two galaxies overlap, providing new constraints on the properties of the young and vigorous extranuclear starburst triggered by the recent interaction of the two galaxies. We use hydrogen recombination lines to derive an extinction of $A_V \approx 70$ to the starburst region, concluding that a model where emitting gas and absorbing dust are mixed best fits the data. We discuss the use of mid-infrared fine structure line ratios for determining the average effective temperature of the stellar ionizing radiation field, and derive an average temperature of 44000 K from the extinction-corrected [Ne III]15.6$\mu$m/[Ne II]12.8$\mu$m line ratio. The observations are well described by starburst models for a recent starburst with an initial mass function extending up to 100 $M_\odot$. Observations of the pure rotational (0-0) S(1) and S(2) lines of molecular hydrogen are used to constrain the fraction of molecular gas that is at temperatures of a few hundred Kelvin.

**Key words:** galaxies: starburst – galaxies: interactions – galaxies: individual: NGC 4038/39 – infrared: galaxies

## 1. Introduction

The two galaxies NGC 4038/39 are probably the best known example of an interacting pair of gas- and dust-rich spirals with collision-induced starburst activity in their overlap region. Because of their relative proximity of 21 Mpc ($H_0$ = 75 km s$^{-1}$ Mpc$^{-1}$), the corresponding large apparent brightness and size, and their extraordinary appearance in the sky, they are well known as a peculiar object 'The Antennae' since the 1940's. Of special interest is the overlap region of NGC 4038/39, for which various observations in the radio (Hummel and van der Hulst, 1986), CO (Stanford et al., 1990), H$\alpha$ (Amram et al., 1992) and optical HST imaging (Whitmore and Schweizer, 1995) provide strong evidence for ongoing extensive star formation. The Infrared Space Observatory ISO (Kessler et al. 1996) offers the opportunity to probe this starburst, which is deeply embedded in giant molecular clouds, at mid- and far-infrared wavelengths. Such observations are much less affected by extinction than optical or near-infrared studies. In this paper we present first results of our ISO-SWS observations of NGC 4038/39.

## 2. Observations

We observed the NGC 4038/39 overlap region in selected emission lines with the SWS *grating line profile scan* mode SWS02 on January 27, 1996. Due to the large angular size of NGC 4038/39 – the nuclei of the two galaxies are separated by more than 1′ – the overlap region can be resolved separately with the SWS apertures of 14″×20″ to 20″×33″ (de Graauw et al. 1996).

Our pointing position R.A. = $12^h01^m54\overset{s}{.}9$, Dec. = $-18°53'04\overset{''}{.}1$ (J2000) was derived from the CO maps of Stanford et al. (1990), where the overlap region appears as one of three bright peaks, the other being the nuclei of the galaxies. The position angle of the SWS aperture, which cannot be influenced by the observer, was $123\overset{\circ}{.}6$. With this orientation, most of the prominent parts of the overlap region, especially the southern clump (cf. Stanford et al., 1990), were covered. However, the nearby nucleus of NGC 4039 is excluded, even for the largest SWS aperture.

In total, 13 fine structure, hydrogen recombination and $H_2$ lines were observed. Ten of them were detected, for the [Fe II], [O IV] and one of the [Ne III] lines we give upper limits. The

*Send offprint requests to*: D. Kunze (kunze@mpe-garching.mpg.de)

⋆ Based on observations made with ISO, an ESA project with instruments funded by ESA member states (especially the PI countries: France, Germany, the Netherlands and the United Kingdom) and with the participation of ISAS and NASA. The SWS is a joint project of SRON and MPE

**Table 1.** Measured line fluxes

| Identification | $\lambda$ $[\mu m]$ | $F_{obs}$ $[W cm^{-2}]$ | Aperture $['' \times '']$ | $\lambda/\Delta\lambda$ |
|---|---|---|---|---|
| H I $Br_\beta$ | 2.626 | $7.25\ 10^{-21}$ | 14×20 | 1400 |
| H I $Br_\alpha$ | 4.052 | $2.18\ 10^{-20}$ | 14×20 | 1500 |
| [Ar III] | 8.991 | $1.56\ 10^{-20}$ | 14×20 | 1700 |
| $H_2$ (0-0) S(2) | 12.279 | $2.81\ 10^{-20}$ | 14×27 | 1200 |
| [Ne II] | 12.813 | $7.97\ 10^{-20}$ | 14×27 | 1300 |
| [Ne III] | 15.555 | $7.35\ 10^{-20}$ | 14×27 | 1700 |
| $H_2$ (0-0) S(1) | 17.035 | $4.72\ 10^{-20}$ | 14×27 | 1800 |
| [S III] | 18.713 | $8.31\ 10^{-20}$ | 14×27 | 2000 |
| [O IV] | 25.890 | $< 5.\ 10^{-21}$ | 14×27 | 1100 |
| [Fe II] | 25.988 | $< 5.\ 10^{-21}$ | 14×27 | 1100 |
| [S III] | 33.480 | $2.80\ 10^{-19}$ | 20×33 | 1100 |
| [Si II] | 34.814 | $2.00\ 10^{-19}$ | 20×33 | 1200 |
| [Ne III] | 36.009 | $< 5.\ 10^{-20}$ | 20×33 | 1250 |
| H I $Br_\gamma$ | 2.166 | $2.08\ 10^{-21}$ [a] | 4.4×31 | |

[a]: measured with IRSPEC on ESO-NTT

observed fluxes are summarized in Table 1. Figure 1 shows the line profiles. The data were reduced with the ISO SWS Interactive Analysis (IA) package, using additional tools for dark subtraction, up-down correction and flat fielding. The results are based on the set of SWS calibration tables as of June 25, 1996. The overall accuracy of the line fluxes is estimated to be $\approx 30\,\%$ (see Schaeidt et al., 1996). In addition, we make use of measurements of the H I Br$\gamma$ line obtained with IRSPEC on the ESO-NTT in June 1992. While the pointing position of the ISO and NTT observations are nearly identical, the size of the apertures and their position angle are rather different. The IRSPEC flux corresponds to a long slit of $4\farcs4 \times 31''$ orientated in the North-South direction.

## 3. Results

### *3.1. Extinction and density of the ionized medium*

The hydrogen recombination lines were used to derive an estimate for the extinction $A_V$, in order to deredden the observed line fluxes. It is necessary to introduce an aperture correction to convert the IRSPEC Br$\gamma$ to the SWS aperture. Since the Br$\gamma$ emission is peaked, we did not scale simply by the factor 2 aperture ratio, but adopted a correction factor 1.6 estimated from our long slit spectrum and the CO map of Stanford et al. (1990).

We have investigated extinction corrections both assuming a simple foreground screen absorber ($F_\lambda = F^0_\lambda\, 10^{-0.4\,A_\lambda}$) and full mix of emitting gas and absorbing dust ($F_\lambda = F^0_\lambda (1 - 10^{-0.4\,A_\lambda})/(0.921\,A_\lambda)$), with $F_\lambda$ being the observed and $F^0_\lambda$ the intrinsic line flux. We minimized the overall scatter of corrected line fluxes with respect to case B for all three lines simultaneously, rather than determining extinctions from individual line ratios and averaging those. Adopting the NIR extinction power law of Mathis (1990), and case B Brackett line ratios of Hummer and Storey (1987) we find that our observations are best fit by a mixed scenario with a visual extinction $A_V \approx 70$, although somewhat different extinctions or screen models in the $A_V \approx 15$ range can be accomodated within the uncertainty of measurements and extinction law. The conclusions drawn below are unaffected by this uncertainty, since the corresponding variations in extinction corrections for the mid-infrared lines are small.

The ratio of the [S III] 18.71$\mu$m/33.48$\mu$m fine structure lines forms an important density diagnostic for the $10^{2.5\,...\,4.5}$cm$^{-3}$ electron density range, with very little dependence on electron temperature. Correcting for extinction and estimating an aperture correction between the apertures used for the two [S III] lines from the CO and radio continuum maps, we infer an electron density of 300 cm$^{-3}$. Because of the slow change with density of the [S III] ratio close to its low density limit, all densities less than 1000 cm$^{-3}$ are consistent with our observations within the uncertainties.

### *3.2. The stellar content of the overlap region*

Line ratios of fine structure lines emerging from different ionization stages of the same element, such as [Ar III]8.9$\mu$m/[Ar II]6.9$\mu$m, [Ne III]15.6$\mu$m/[Ne II]12.8$\mu$m and [S IV]10.5$\mu$m/[S III]18.7$\mu$m, depend strongly on the properties of the ionizing radiation field while being independent of abundances and only mildly extinction-dependent. The photoionization code CLOUDY (version 84.12a, Ferland 1993) was used to compute theoretical values for these line ratios for various sets of EUV input flux distributions. We have updated some of the atomic data used by CLOUDY, the only change significant for this work being an updated [Ar II]6.9$\mu$m collision strength (Pelan & Berrington 1993). The dependencies of the line ratios on the ionizing radiation field can be summarized in diagnostic plots (see Fig. 2), from which the properties of the radiation field can easily be derived by comparison with observation. We used spectral energy distributions from photospheric LTE model atmospheres by Kurucz (1994) and recent NLTE calculations by Sellmaier et al. (1996), which include radiative-driven wind theory as well as a consistent treatment of the NLTE line blocking opacities. An ionization parameter of $\log(U) = -2.5$ was adopted for starbursts from the measured electron density and Lyman continuum luminosity under the assumption that the typical source sizes are comparable to the overall size of the starbursts. Solar abundances were assumed.

From the [NeIII]15.6$\mu$m/[NeII]12.8$\mu$m ratio of 0.8 (including a small extinction correction) we deduce a single star equivalent effective temperature of 44000 K. The resulting temperature is independent of the use of Kurucz or Sellmaier flux distributions (see Fig. 2). It should however be pointed out that for the [S IV]/[S III] and [Ar III]/[Ar II] ratios and also for the [NeIII]/[NeII] ratio at different temperatures, the adopted flux distribution has a significant effect on the deduced line ratios (Fig. 2). The reason for this are considerable differences between the flux distributions from the most recent NLTE model atmospheres and previous LTE calculations, for which we give

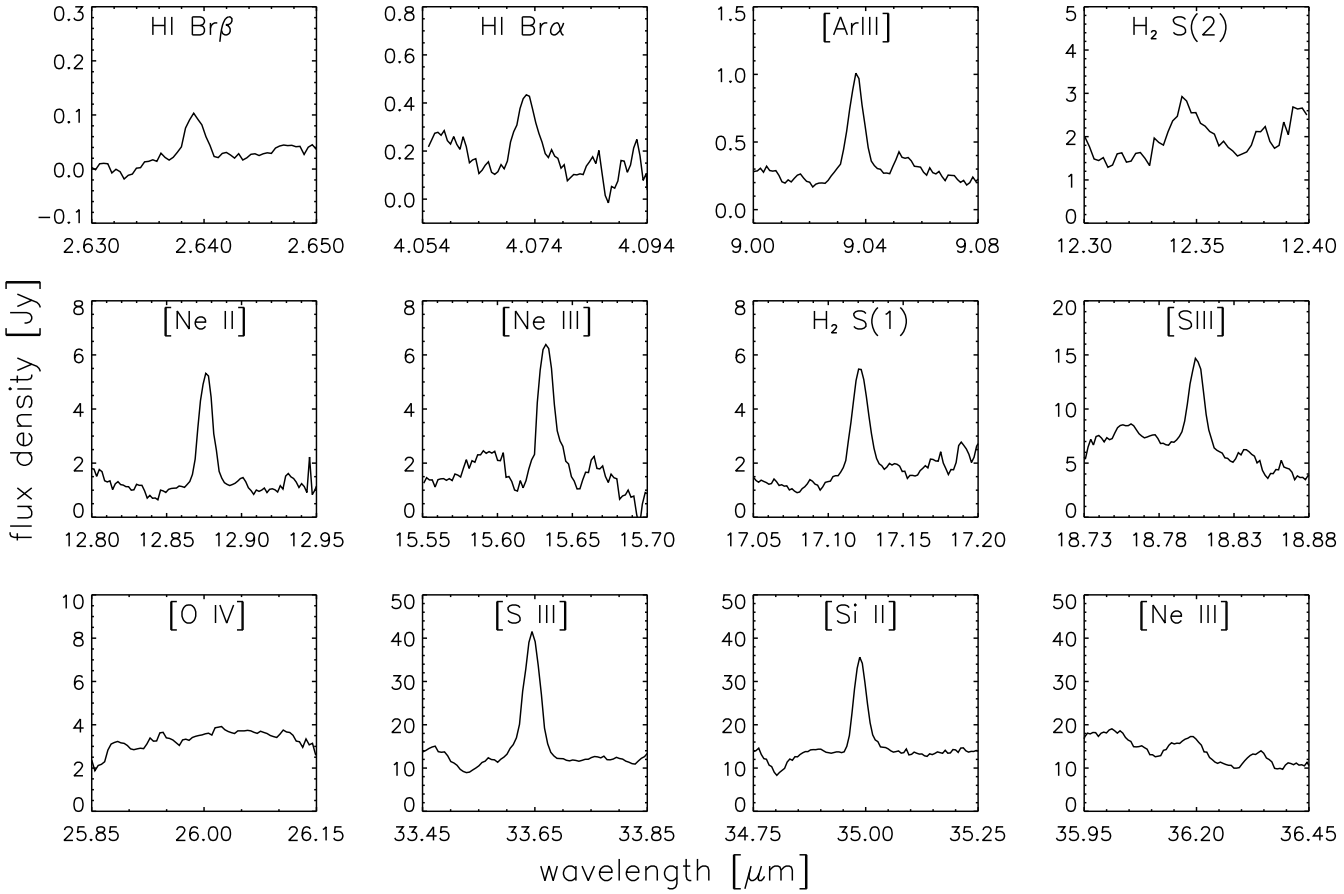


**Fig. 1.** The SWS line spectra of the NGC 4038/39 overlap region

an example in Fig. 3, indicating also the ionization edges for the creation of some species emitting important mid-infrared fine structure lines.

The effective temperature of 44000 K corresponds to an O5 main sequence star with a mass of 50-60 $M_\odot$. However, a single star spectrum is only a crude approximation to the combined ionizing radiation field of the variety of OB stars in an evolving starburst. Even in the highly simplified case of a zero age main sequence populated according to an $\alpha = -2.40$ Salpeter initial mass function (IMF), the mixed stellar radiation field will be softer than for its most massive stars. Therefore we synthesized combined spectra for different upper mass cutoffs by integrating single star spectra, weighted according to their contribution to the Salpeter IMF. CLOUDY was then used to derive the dependency of the line ratios on the upper mass cutoff. The best fit to our observed [NeIII]/[NeII] ratio is an upper mass cutoff of 65 $M_\odot$. This can be considered a lower limit to the actual upper mass cutoff in an evolving starburst, since evolution will rapidly soften the radiation field.

A more adequate treatment is to use a star cluster evolution code (Kovo and Sternberg 1996) to derive the correct weighting of stellar atmospheres for input to the photoionization code (in this case we used ION, Netzer (1993)). For NGC 4038/39 and other starbursts we observed to date with SWS, fine structure line ratios and global quantities can be fit with plausible star forming histories and IMFs extending to high masses (see Lutz et al. (1996), who also present model output in their Fig. 3). In the case of the Antennae overlap region, a young ($\approx 7 \times 10^6$ yr) starburst with IMF extendening up to 100 $M_\odot$ provides a good

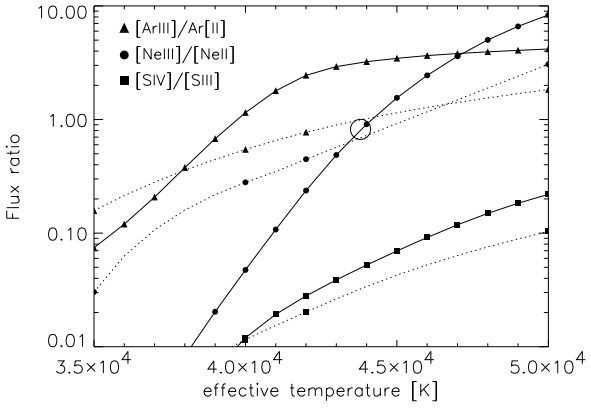


**Fig. 2.** Diagnostic plot of fine structure line ratios versus effective temperature of the ionizing spectrum derived from Kurucz (1994, solid) and Sellmaier et al. (1996, dotted) atmospheres. The open circle indicates the measured [NeIII]/[NeII] ratio for NGC 4038/39.

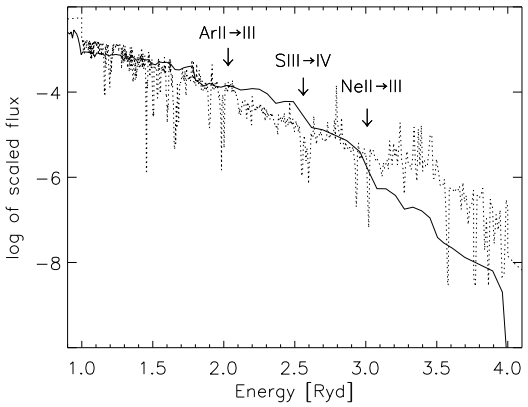


**Fig. 3.** Comparison between normalized stellar EUV flux distributions from models by Kurucz (1994, solid) and Sellmaier et al. (1996, dotted) for $T_{eff}$ = 40000 K. Some ionization edges relevant for the strength of mid-infrared fine structure lines are indicated.

fit to all observational constraints. The combined cluster evolution code / photoionization code models demonstrate that excitation measures like [Ne III]/[Ne II] drop significantly already during the first few million years of starburst evolution. Thus, constraints on the upper IMF cutoff based on zero-age main sequence populations indeed impose too strict upper mass cutoffs.

### *3.3. Molecular Hydrogen Emission*

ISO-SWS offers the unique opportunity to probe the bulk constituent of warm molecular material by observing the pure rotational lines of molecular hydrogen. For this initial observation of NGC 4038/39, we included the 17.03$\mu$m S(1) and 12.28$\mu$m S(2) lines. Both lines are detected, with the S(2) flux being somewhat uncertain due to residual fringing caused by the complex and source-dependent structure of the SWS band 3 relative spectral response function. Assuming that the involved levels are thermalized ($n > 10^4\,\mathrm{cm}^{-3}$) and for an ortho-para ratio of 3, we infer a temperature of 405 K from the S(2)/S(1) ratio, warmer than inferred from the same ratio in other starburst galaxies observed with SWS to date (e.g. Rigopoulou et al., 1996). The temperature spread of molecular gas causes the temperature deduced from S(2)/S(1) to be higher than the average temperature of S(1) emitting gas (Egami et al. 1996). If we tentatively adopt a temperature of 200 K we can estimate a mass of $5.6 \times 10^7\,\mathrm{M}_\odot$ for this warm molecular phase. The warm molecular gas, which may be produced in shocks or PDRs associated with the star formation activity, then constitutes $\approx$8% of the total $H_2$ mass of $7.3 \times 10^8\,\mathrm{M}_\odot$ that Stanford et al. (1990) deduce from their CO measurements for the southern clump. Changing the adopted temperature to 405 K, as directly obtained from the S(2)/S(1) ratio would lower the estimated warm molecular mass by a factor 7.

*Acknowledgements.* This research has made use of the NASA/IPAC Extragalactic Database (NED). SWS and the ISO Spectrometer Data Centre at MPE are supported by DARA under grants 50 QI 8610 8 and 50 QI 9402 3. SWS acknowledges contributions from KULeuven, Steward Obs. and Phillips Lab. This work has been partly supported by the German-Israel Foundation grant I-196-137.7/91.

## References

Amram P., Marcelin M., Boulesteix J., le Coarer E., 1992, A&A, 266, 106
de Graauw Th., Haser L., Bauer O.H., et al., A&A, 1996, this issue
Egami E., et al., 1996, in prep.
Ferland G.J., 1993, Dep. of Physics and Astronomy Internal Report, Univ. of Kentucky
Kurucz R.L., 1994, Smithonian Astrophysical Observatory, Kurucz CD-ROM No. 19
Hummel E., Van der Hulst J.M., 1986, A&A, 155, 151
Hummer D.G., Storey P.J., 1987, MNRAS, 224, 801
Kessler M.F., et al., 1996, A&A, this issue
Kovo O., Sternberg A., 1996, in preparation
Lutz D., Genzel R., Sternberg A., et al., 1996, A&A, this issue
Mathis J.S., 1990, ARA&A, 28, 37
Netzer H., 1993, ApJ, 411, 594
Pelan J., Berrington K.A., 1995, A&AS, 110, 209
Rigopoulou D., Lutz D., Genzel R., et al., 1996, A&A, this issue
Schaeidt S., Morris P., Salama A., et al., 1996, A&A, this issue
Sellmaier F.H., Yamamoto T., Pauldrach A.W.A., Rubin R.H., 1996, A&A, 305, L37
Stanford S.A., Sargent A.I., Sanders D.B., Scoville N.Z., 1990, ApJ, 349, 492
Whitmore B.C., Schweizer F., 1995, AJ, 109, 960